Available online at www.sciencedirect.com
SCIENCE DIRECT®
Journal of Sound and Vibration 267 (2003) 575–589
JOURNAL OF SOUND AND VIBRATION
www.elsevier.com/locate/jsvi

Prediction and measurements of vibrations from a railway track lying on a peaty ground

B. Picoux[a,*], R. Rotinat[b], J.P. Regoin[a], D. Le Houédec[a]

[a] *Ecole Centrale of Nantes, LMM, 1 rue de la Noë, BP 92 101, 44321 Nantes Cedex 3, France*
[b] *University of Orléans, LMSP, 8 rue Léonard de Vinci, 45072 Orleans Cedex 2, France*

Accepted 9 May 2003

Abstract

This paper introduces a two-dimensional model for the response of the ground surface due to vibrations generated by a railway traffic. A semi-analytical wave propagation model is introduced which is subjected to a set of harmonic moving loads and based on a calculation method of the dynamic stiffness matrix of the ground. In order to model a complete railway system, the effect of a simple track model is taken into account including rails, sleepers and ballast especially designed for the study of low vibration frequencies. The priority has been given to a simple formulation based on the principle of spatial Fourier transforms compatible with good numerical efficiency and yet providing quick solutions. In addition, in situ measurements for a soft soil near a railway track were carried out and will be used to validate the numerical implementation. The numerical and experimental results constitute a significant body of useful data to, on the one hand, characterize the response of the environment of tracks and, on the other hand, appreciate the importance of the speed and weight on the behaviour of the structure.

1. Introduction

Along a railway track in the North West of France, observations revealed the existence of high displacements of the ground surface during the passage railway traffic. These vibrations are greatest, and therefore more damaging to the ground surrounding the track and to the track itself, when the speed and the weight of the train are large, particularly when the speed of the train exceeds the low speed of surface waves in soft ground. These vibrations cause high displacements in the track (mainly for the rail) which are not acceptable for the safety and the speed of the

*Corresponding author.
E-mail address: benoit-picoux@ec-nantes.fr (B. Picoux).

0022-460X/$ - see front matter © 2003 Elsevier Ltd. All rights reserved.
doi:10.1016/S0022-460X(03)00725-9

railway traffic. Long-term effects are possible for the track foundations, the rail or for neighbouring structures. Aware of these problems, the French Ministry of Environment has financed a research programme to study railway noise and vibrations. This research is intended to increase understanding of the phenomenon of vibration propagation from railway vehicles moving at high and constant speed. The project partnership includes the French National Railway and a European geophysical company. The first objective consists of developing simulation and estimation methods for vibrations near the track. The study of a simple two-dimensional model of track–soil interaction then enables resonance frequencies of the system and the critical speed of the train to be determined. A parametric analysis of the track components and the ground parameters is also performed. Effects of modification of the track can also be studied (strengthening of the foundation by adding rails, reduction of the distance between sleepers). Secondly, in situ measurements have been undertaken in order to validate the modelling and to obtain useful and suitable data to understand the phenomena of wave propagation from vehicles, especially trains, moving at constant speed. This final part of the study is still in progress and only the results of the initial part of the study are presented here.

2. Prediction model

The phenomena of wave propagation in the ground have previously been the subject of considerable research [1], with associated numerical simulations [2] and in situ measurements [3]. In these analyses, mechanical characteristics and behaviour laws of the different soils play an important part in determining the relevance and the validity of the proposed model [4]. Therefore hypotheses have to be chosen with care. For some decades, the speed of the moving load has been recognized as an essential factor in determining wave propagation at the surface of the ground [5], or possibly underground (for example tunnels). The value of this speed is compared to that of the Rayleigh wave. This type of wave plays a dominant role in the observable vibration amplitude [6] during the passage of a train.

In this study, a two-dimensional model is assumed. It represents a cross-section below the track. Since the load moves at constant speed along the Ox-axis and displacements are studied in the Oxz plane, the assumption of plane strain in each direction perpendicular to the track is assumed. So this problem could be reduced to a two-dimensional one since every plane perpendicular to Oy is a symmetry plane. With this approximation, the model allows one to study the displacement field at the soil surface.

A railway track model [7] lying on a layered soil medium and subjected to a railway traffic can be developed using the formalism of the Fourier transform [2]. Fig. 1 illustrates the complete model with two distinct parts: the rail lying on sleepers connected through railpads, the ground comprising the ballast and n layers. A fixed reference point linked to the ground and a moving reference point linked to the single and rectangular harmonic load are denoted respectively by (O, x_1, x_3) and (O, x, z). A parametric analysis of the different track elements and a vertical displacement evaluation according to the speed and the composition of trains can be given by this model.

The rail is represented as an infinite Euler beam with the following characteristics: mass per unit length m_R, Young's modulus E and second moment of area I. Railpads and sleepers are

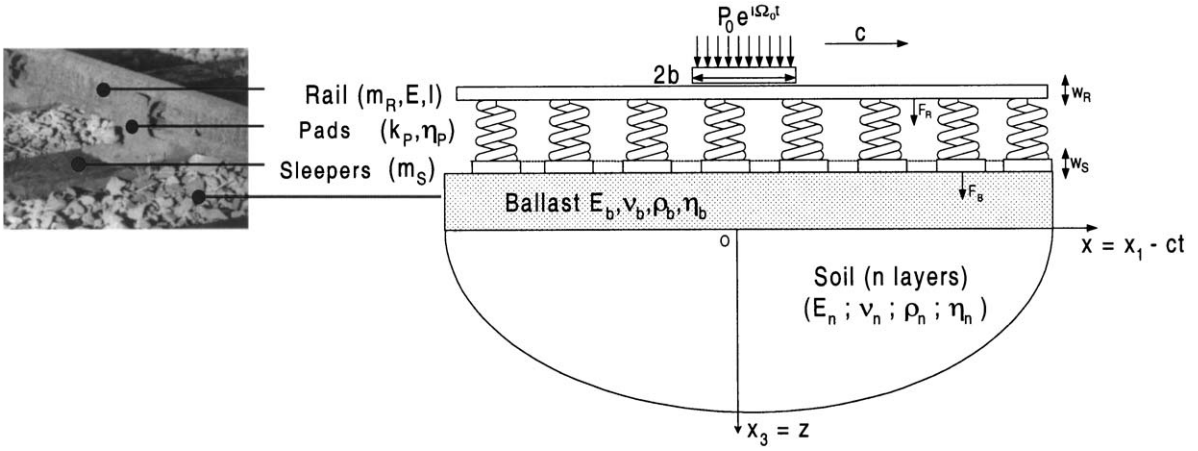

Fig. 1. Description of prediction model.

represented as a continuous mass–spring system [2], (mass per unit length m_S, stiffness per unit length k_P and damping η_P). For this kind of use of a continuous support is justified taking into account the wavelengths studied (frequency range less than 100 Hz).

For the rail described by an Euler beam [2], the following equation is obtained:

$$EI\frac{\partial^4 w_R(x_1,t)}{\partial x_1^4}+m_R\frac{\partial^2 w_R(x_1,t)}{\partial t^2}+k_P[w_R(x_1,t)-w_S(x_1,t)] = \begin{cases}\sigma_{TRAIN}(x_1,t) & \text{if } |x_1-ct|<b,\\ 0 & \text{else,}\end{cases} \tag{1}$$

where $\sigma_{TRAIN}(x_1,t)$ is the Cauchy stress applied by the train, equal to $P_0 e^{i\Omega_0 t}/2b$ for a harmonic rectangular load (Fig. 1). w_R and w_S represent respectively the vertical displacements of rail and sleepers. F_R is the force exerted by the rail on the sleepers.

The equation for the sleepers is written as follows:

$$m_S\frac{\partial^2 w_S(x_1,t)}{\partial t^2}+k_P[w_S(x_1,t)-w_R(x_1,t)]=-F_B(x_1,t), \tag{2}$$

where F_B is the force exerted on the ballast which provides the contact between the structure and the layered ground.

This structure is lying on a multi-layered ground. The thickness of layer n is h_n. The first layer represents the ballast (mechanical parameters: E_b, ν_b, ρ_b, η_b). Below the ballast, each soil layer is described by its mechanical parameters E_n, ν_n, ρ_n, η_n. Under the lowest layer a halfspace is assumed.

For an elastic, homogeneous and isotropic layer, the equation of motion is

$$(\lambda+\mu)\nabla(\nabla\cdot U)+\mu\Delta^2 U=\rho\frac{\partial^2 U}{\partial t^2}, \tag{3}$$

where U is the vector of displacements and λ, μ are the Lamé's constants, and for the behaviour law:

$$\sigma_{ij} = \lambda\delta_{ij}(\nabla \cdot U) + \mu\left(\frac{\partial u_i}{\partial x_j} + \frac{\partial u_j}{\partial x_i}\right). \tag{4}$$

To define elastic body waves (P- and S-waves), Helmholtz's potentials ϕ and ψ are usually used, so that

$$U = \nabla\phi + \nabla \wedge \Psi. \tag{5}$$

The typical train excitation is composed of a set of vertical components that symbolize the effect of each engine and carriage wheel on the rail. Each of these forces is taken as harmonic. The solution method [6] is illustrated in Fig. 2. The "fitted phase angle" is defined by Helmholtz's potentials, so that

$$\begin{cases} \phi = A\mathrm{e}^{\alpha_P(z-h)} + C\mathrm{e}^{-\alpha_P z} \\ \psi = B\mathrm{e}^{\alpha_S(z-h)} + D\mathrm{e}^{-\alpha_S z} \end{cases} \quad \text{where } \alpha_i = \sqrt{\beta^2 - \frac{\Omega_0 - \beta c}{c_i}},\ i = P, S, \tag{6}$$

where $c_P(E, \rho, v)$ is the speed of compression waves (P-waves) and $c_S(E, \rho, v)$ the speed of shear waves (S-waves) (examples of such parameters, used in Section 3, are given in Table 1). Because of numerical difficulties due to exponential terms in the rigidity matrix, layers must be divided into several sub-layers increasing the number of iterations. In fact, the role of the fitted phase

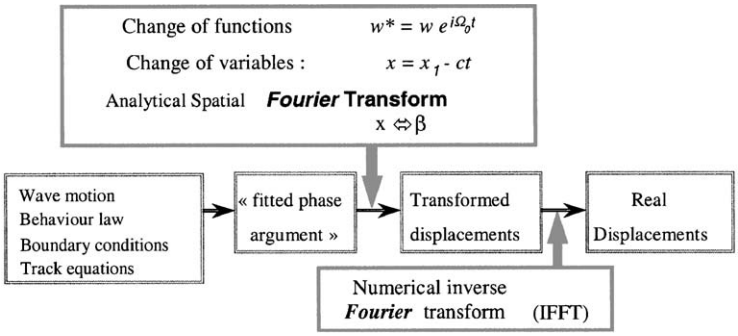

Fig. 2. Resolution method.

Table 1
Parameters for numerical investigation

	h (m)	E (N/m^2)	v	ρ (kg/m^3)	η	c_P (m/s)	c_S (m/s)
Ballast	0.8	300×10^6	0.3	1800	0.1	547	292
Layer	7	269×10^6	0.257	1550	0.1	459	263
Substratum	∞	2040×10^6	0.179	2450	0.1	950	594

translation is to solve this problem by excluding exponential terms (growing exponential) in the stiffness matrix thus providing good conditioning.

A change of variables (translation in the mobile reference linked to the load) and functions (evaluation of the steady state solution) as well as the use of spatial Fourier transform lead to the calculation of vertical displacements in the wave number domain (Fig. 2).

After writing equations concerned with the wave motion, the behaviour law, the boundary conditions for each layer [3] and track equations [2], a relationship between displacements and stresses at each layer interface (including the ballast) can be written.

This relationship is given in a matrix form as

$$\begin{bmatrix} T_{11}^{Bal} & T_{21}^{Bal} & T_{31}^{Bal} & T_{41}^{Bal} & 0 & 0 \\ T_{12}^{Bal} & T_{22}^{Bal} & T_{32}^{Bal} & T_{42}^{Bal} & 0 & 0 \\ T_{13}^{Bal} & T_{23}^{Bal} & T_{33}^{Bal}+T_{11}^{n} & T_{43}^{Bal}+T_{21}^{n} & T_{31}^{n} & T_{41}^{n} \\ T_{14}^{Bal} & T_{24}^{Bal} & T_{34}^{Bal}+T_{12}^{n} & T_{44}^{Bal}+T_{22}^{n} & T_{32}^{n} & T_{42}^{n} \\ 0 & 0 & T_{13}^{n} & T_{23}^{Bal} & T_{33}^{n}+R_{11} & T_{43}^{n}+R_{21} \\ 0 & 0 & T_{14}^{n} & T_{24}^{Bal} & T_{34}^{n}+R_{12} & T_{44}^{n}+R_{22} \end{bmatrix} \begin{Bmatrix} \mathrm{i}\bar{w}_{z=0}^{*}(\beta) \\ \bar{u}_{z=0}^{*}(\beta) \\ \mathrm{i}\bar{w}_{z=h}^{*}(\beta) \\ \bar{u}_{z=h}^{*}(\beta) \\ \mathrm{i}\bar{w}_{z=h^n}^{*}(\beta) \\ \bar{u}_{z=h^n}^{*}(\beta) \end{Bmatrix} = \begin{Bmatrix} -\mathrm{i}\bar{\sigma}_{zz}^{*}(\beta) \\ -\bar{\sigma}_{xz}^{*}(\beta) \\ 0 \\ 0 \\ 0 \\ 0 \end{Bmatrix} = \begin{Bmatrix} \mathrm{i}\bar{F}_{S}^{*}(\beta) \\ 0 \\ 0 \\ 0 \\ 0 \\ 0 \end{Bmatrix}, \tag{7}$$

where * indicates the change of function and $\bar{w}$ the Fourier transform of w. This matrix is built by writing relationships between stresses and displacements at the interface of each layer [2]. $[T^{Bal}]$ is the stiffness matrix of ballast, $[T^n]$ is the stiffness matrix of n ground layers and $[R]$ is the stiffness matrix of the halfspace. The stiffness matrix $[T]$ is obtained by forming the product of the inverse of the displacement matrix $[Q]$ with the stress matrix $[S]$, whose coefficients depend on Lamé coefficients, layer thickness h, excitation frequency Ω_0, load speed c, and wave number β. All these coefficients are complex because of hysteretic damping considered in the model.

Thus, vertical displacements at the surface of the ballast and of the ground can be written, respectively, as

$$\bar{w}_{z=0}^{*}(\beta) = [T]_{11}^{-1}\bar{F}_{S}^{*}(\beta) \quad \text{and} \quad \bar{w}_{z=h}^{*}(\beta) = [T]_{31}^{-1}\bar{F}_{S}^{*}(\beta). \tag{8}$$

By assuming that the system of sleepers is continuous, which is reasonable for the wavelengths involved, the system can be written in the following equations:

$$\begin{cases} (EI\beta^4 - m_R\Omega_0^2 + k_P)\bar{w}_{R}^{*}(\beta) - k_P\bar{w}_{S}^{*}(\beta)] = \bar{\sigma}_{TRAIN}(\beta), \\ -k_P\bar{w}_{R}^{*}(\beta) + (k_P - m_S\Omega_0^2)\bar{w}_{S}^{*}(\beta) = -\bar{F}_{S}^{*}(\beta), \\ \bar{w}_{S}^{*}(\beta) = [T]_{11}^{-1}\bar{F}_{S}^{*}(\beta) \end{cases} \tag{9}$$

from which the displacements at the soil surface can be obtained:

$$\bar{w}^*_{z=h}(\beta) = [T]^{-1}_{31}\frac{k_P\bar{\sigma}_{TRAIN}(\beta)}{[(EI\beta^4 - m_R\Omega_0^2 + k_P)(k_P - m_S\Omega_0^2) - k_P^2][T]^{-1}_{11} + (EI\beta^4 - m_R\Omega_0^2 + k_P)}. \quad (10)$$

Then $\bar{w}^*_{z=h}(\beta)$ represents the vertical displacement in the wave number domain under the ballast (ground surface). An analytical solution exists if the soil is considered as infinite in the positive z direction. In this case, the Rayleigh's function involving an infinite vertical displacement is obtained by the cancellation of the denominator, deducing exactly the speed of *Rayleigh* waves in the medium [1]. Then, a residual method by integration in the complex plane gives the actual vertical displacements. In the case of a layered soil, actual displacements are calculated numerically by an inverse Fourier transform.

3. Numerical results

For the numerical simulations, the following data have been used for the structure. First, for the steel rail, the Young's modulus is 2.11×10^{11} N/m^2, the second moment of area is 3055 cm^4 and the mass per unit length of track length is 120 kg/m. The stiffness of the pads between the rail and sleepers is 3.5×10^8 N/m with a damping coefficient equal to 0.15. The mass of sleepers per unit of track length is 490 kg/m.

For the numerical investigation the case of a relatively soft multi-layered soil is considered first (before considering a peaty soil). In the following example, a 7 m soft layer is lying on a halfspace. Mechanical parameters for this example are summarized in Table 1.

First, a harmonic unit load (40 Hz) is assumed to be acting on the rail surface. In Fig. 3, maximum displacements at the soil surface are plotted for the conceivable speed regimes ("static" $c = 0$, sub-Rayleigh $c = 0.5 \times C_R$ and super-Rayleigh $c = 1.5 \times C_R$). These displacements are

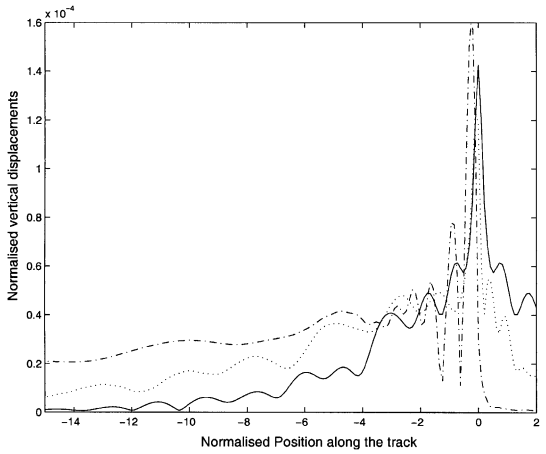

Fig. 3. Maximum displacements for the three speed regimes ($c = 0$: dashed line, $c = 0.5 \times c_R$: dash-dotted line, $c = 1.5 \times c_R$: solid line).

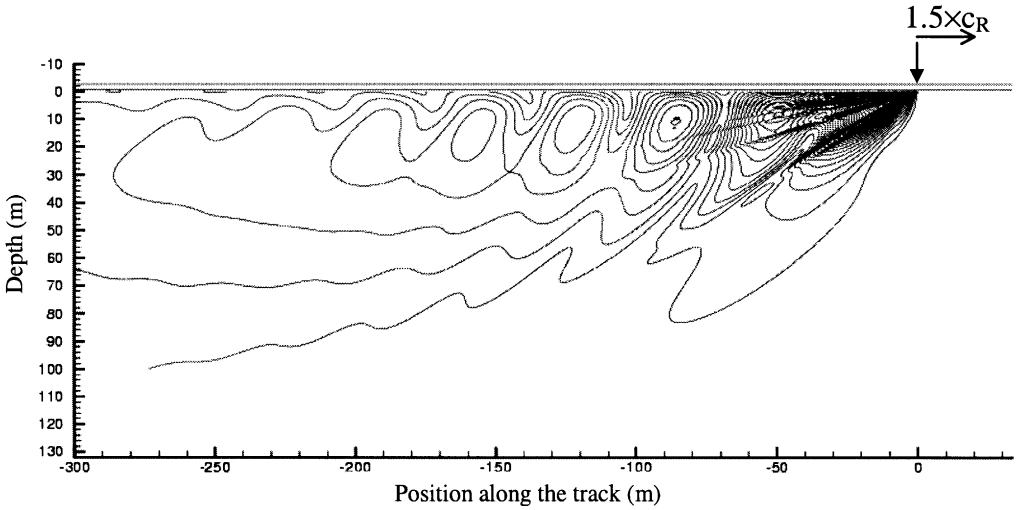

Fig. 4. Contours of displacements against depth in super-Rayleigh regime.

symmetrical relative to the load when the speed is zero. Larger amplitudes are obtained when the load is moving. For the super-Rayleigh regime, displacements behind the load are greater and oscillating. In this last regime Mach cones are observed in the presence of wave fronts moving with the load. These cones are due to the P- and S-waves and exist in the ground (Fig. 4) but also at the soil surface due to the dominant R-waves.

Then, an excitation by a series of harmonic loads representing the train loading is considered. Here, only the effect of the dynamic force is considered. In fact, real excitation is the summation of the static part (weight mg) and the dynamic part (harmonic force).

The analytical expression of stress for a train can be written easily in the wave number domain thanks to symmetries observer previously. Fig. 5 presents the vertical stress function (Cauchy stress) for a typical "Corail" train composed of an engine and two carriages. This function, involving the same low excitation frequency for all loads (wheels), is introduced in the model of track–soil interaction. A "Corail" train has a diesel locomotive pulling two passenger cars. However an "Autorail" train is a multiple unit passenger diesel train.

Displacements generated at the ground surface by the train are plotted in Fig. 6 according to the different speed regimes.

When the train is stationary on the track, the ground undergoes a displacement due to the train loading on the track (static regime). The appearance of the curve obtained for this regime remains until the speed is equal to about 0.5 times the speed of the surface Rayleigh wave. The moving load leads to larger vibrations in front of and behind the wheel load (sub-Rayleigh regime) but only behind the wheel load (super-Rayleigh regime).

Finally, the model developed allows one to evaluate numerically vertical, longitudinal and lateral displacements for all points on the ground surface and at the interface of each layer as well as the vertical displacement of each track element.

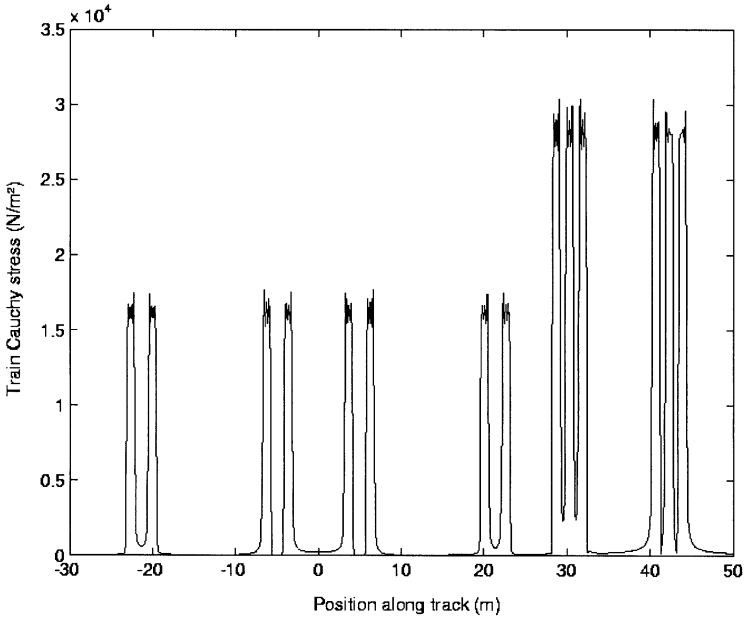

Fig. 5. Actual train Cauchy stress σ_{TRAIN} for a current French train.

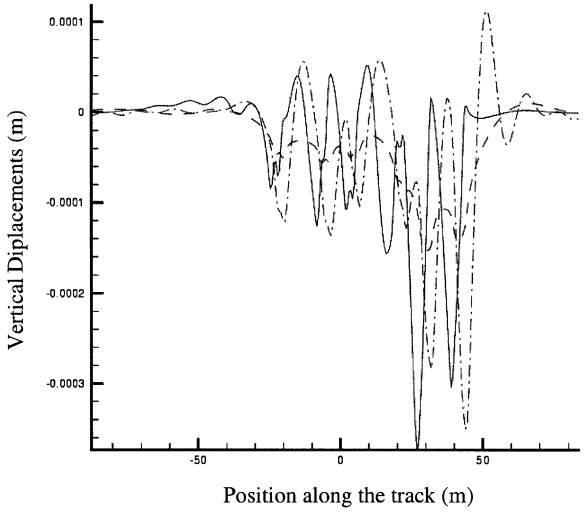

Fig. 6. Maximum vertical displacements at the soil surface near the track for current train ($c = 0$: dashed line, $c = 0.5 \times c_R$: dash-dotted line, $c = 1.5 \times c_R$: solid line).

4. Experimental investigations

In addition to the simulation studies, in situ measurements have been undertaken in partnership with the French National Railway (S.N.C.F.) and a geophysical company (Soletanche-Bachy).

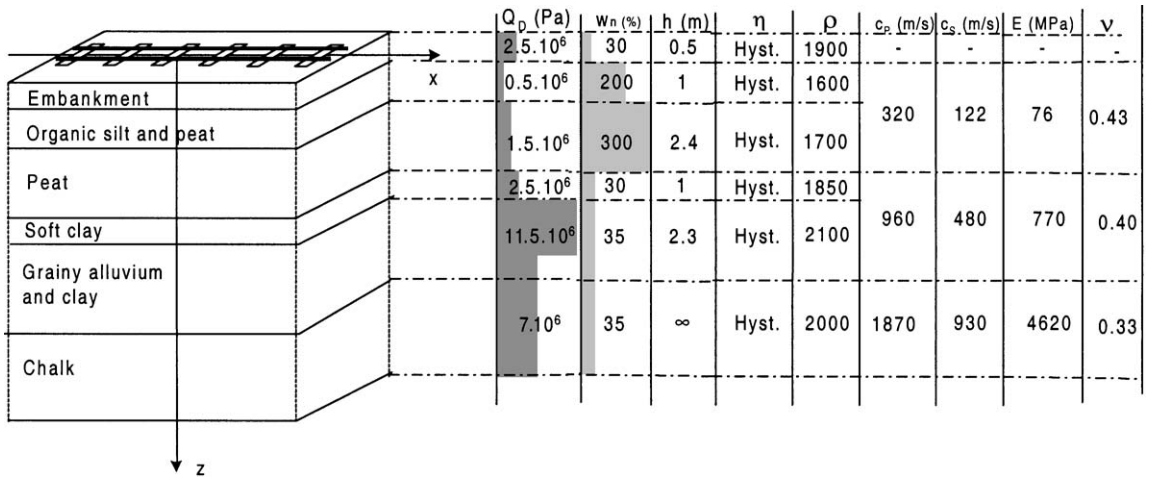

Fig. 7. Characteristics of the ground.

The three sites studied are situated in the valley of the River Somme along the Amiens–Boulogne (France) railway line and are concerned with different situations (current track with vibration problems, modified track with vibration problems, current track without vibration problem). These sites correspond to a ground composed of a peaty and clayey soil (a few metres deep) lying on a limestone substratum (Fig. 7).

A sounding test indicated a deep layer of saturated soil (saturated as a consequence of floods during the spring 2001). A parameter study of the ground undertaken by seismic measurements shows a critical speed close to 100 m/s (Rayleigh wave speed) while the trains studied travelled at sub-Rayleigh speeds (20–50 m/s).

For the two problematical sites, during the passage of a heavy train, the railway formation and the ground undergo displacements in the order of some millimeters (with a maximum displacement of 10 mm possible at the rail). The railway structure is composed of a rail UIC60, bi-block sleepers U41, pads and ballast. Measurements were performed at the end of July 2001 for the three sites, the measurement related to vibrations being coupled with other tests with the aim to determine the mechanical characteristics of ground. The measurements have provided much information about lateral and vertical accelerations of track elements and of the soil surface. With the help of a fast digital camera, a Laser velocimeter, and several accelerometers, all displacements could be evaluated for each loading and for different speeds. The measurement positions are indicated in Fig. 8.

To evaluate in situ rail vibrations, an experimental device was developed. Coupled with an accelerometer and a velocimeter, an optical technique was used to measure the in-plane displacement. This method was based on the tracking of markers which are simply deposited with a felt pen or painted on a surface (see Fig. 9). A high-speed CCD video camera (Motion Vision CA-D6) with a 532×512 pixel spatial resolution and a data acquisition card associated with a software (SYSMAT Industries VNR250) was used to monitor the surface studied, to transfer and to record the corresponding images to a Personal Computer. With this arrangement, the maximum acquisition frequency is 250 frames/s. In this case, the acquisition time was close to 7 s; that is, approximately 1800 images.

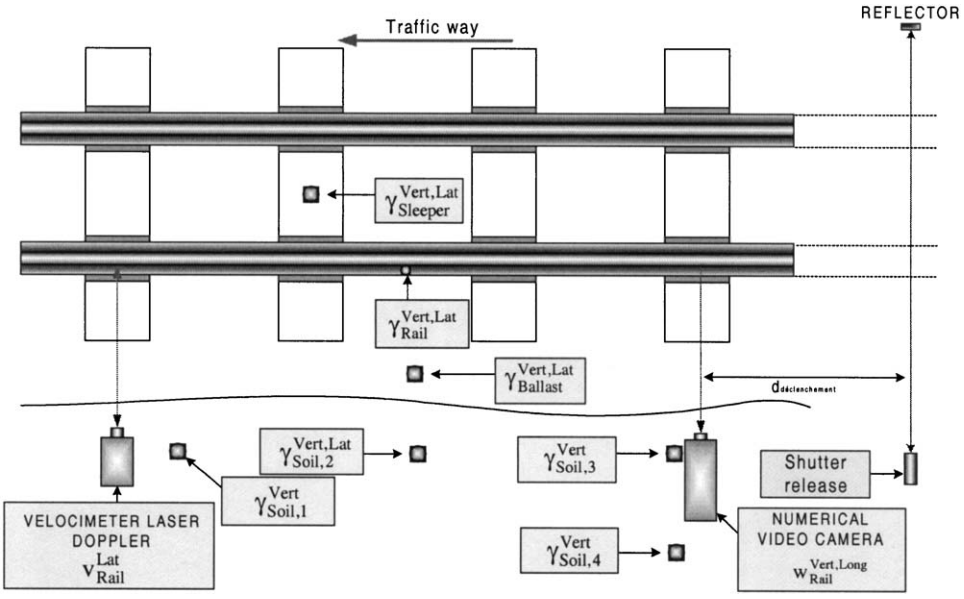

Fig. 8. Description of experimental investigation.

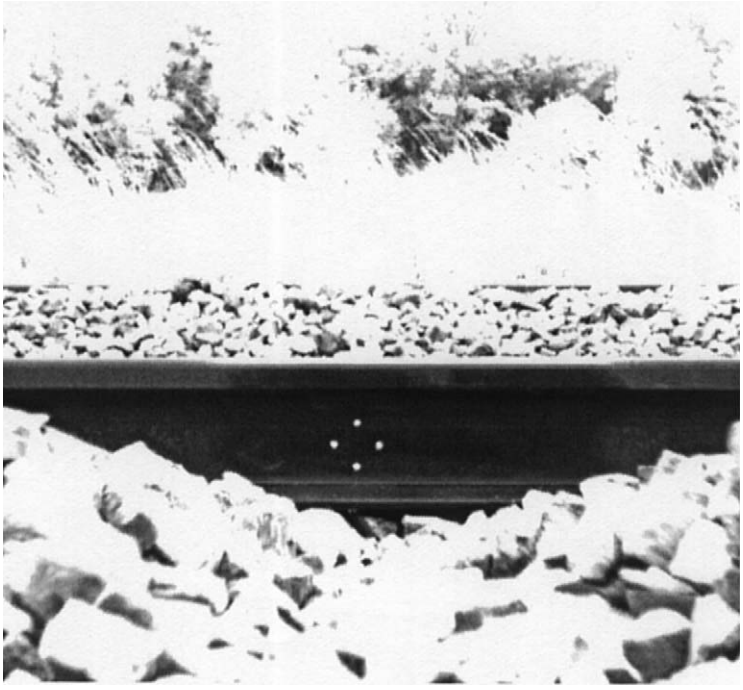

Fig. 9. Picture from the fast numerical video camera.

The device enabled longitudinal and vertical displacements of the rail to be measured as well as deformations. Also an accurate value of the train speed can be obtained thanks to an infrared detector cut by the traffic. As the camera was fixed in the vicinity of the track (2 m), an accelerometer was laid on the ground near the latter in order to correct displacements transmitted from the ground to the optical system. The Laser velocimeter provided indications of lateral rail displacements (due to a light track curve). An accelerometer was attached to the rail by a magnetic base and was used in a vertical or lateral position to confirm previous results. Another accelerometer was glued to a sleeper and allowed some information to be determined on the behaviour of the pads. Finally five accelerometers were mounted on the ground and the ballast. Distances between each of them can vary from one site to another (function of estimated wavelengths and possibility of arrangement).

Altogether, at the three sites, measurements were obtained for about 30 trains, offering a parametric diversity taking into account the speed of the train and the traffic type (freight, "Autorail" or "Corail").

5. Experimental results

Displacements of each track element and displacements on the soil surface were calculated with a reasonable accuracy from the recorded accelerations. Particular attention was paid to the test procedure, the transducers used to record the accelerations and the test parameters such as the sample rate.

Thanks to an asynchronous recording between the numerical and analogue channels, a sample rate of 1000 samples per second was used. So the acceleration data from accelerometer measurements could be integrated successfully to obtain velocity and displacement data using two numerical integrations.

A small DC offset was observed in the data due to the bias in the signal conditioning and this caused a linear trend in the velocity results as well as in the displacement results. Consequently, digital filters were used carefully to remove extraneous errors to the signals. For all measurement data, the trend was removed by using a high-pass Butterworth filter before each integration.

The analysis of all images of the form of Fig. 9 was performed in delayed time thanks to a program which automatically calculated for each image the mark centre and their positions. The localization of the centre was done by the calculation of the mark barycentre weighted by the light intensity. The lower limit of the light intensity must be chosen in order to extract correctly the mark from the background. The accuracy is a function of the mark diameter. Local plane rail displacements were finally and easily deduced from co-ordinates of the marks. Results of this analysis for a Corail train passage at two different speeds are plotted in Fig. 10. At 70 km/h, vertical rail displacements (max. 3 mm) are smaller than for 135 km/h (max. 9 mm) and are only quasi-static (deformation under each wheel).

Fig. 11 shows displacements (absolute mean value) of each track element against the type of traffic. Note that, in each element, displacements are greater for heavy traffic like a Corail train. Also, this figure gives an evaluation of attenuation between track elements. Finally Fig. 12 shows the shape and amplitude of displacements at the soil surface at two points perpendicular to track

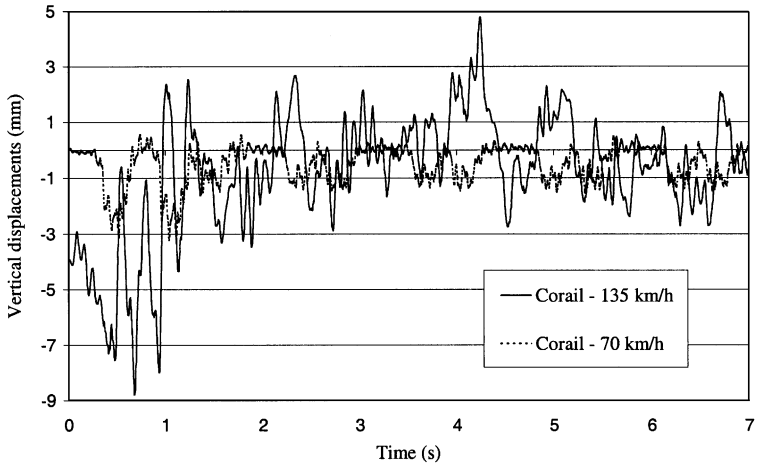

Fig. 10. Vertical displacements measured by numerical video camera ("Corail" train composed of two engines and six carriages).

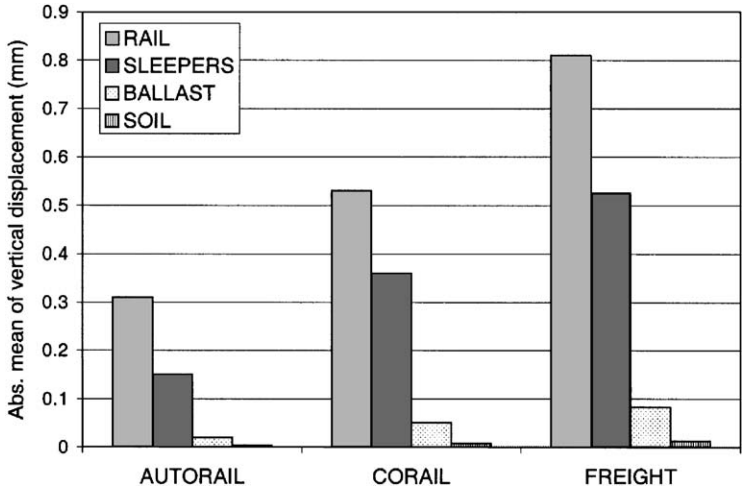

Fig. 11. Vertical displacements of track elements for different traffic passages.

near the embankment. Maximum displacements (peak to peak) are then about 1 mm (already significant for this low train speed).

6. Validation

Measured P- and S-wave speeds for the peat are respectively 262 and 193 m/s while for the limestone substratum they are 1878 and 915 m/s. For this soft layer resonance frequencies are obtained leading to higher displacements. These natural frequencies can be calculated approximately and depend on the P- and S-waves speeds in the layer and on the layer thickness.

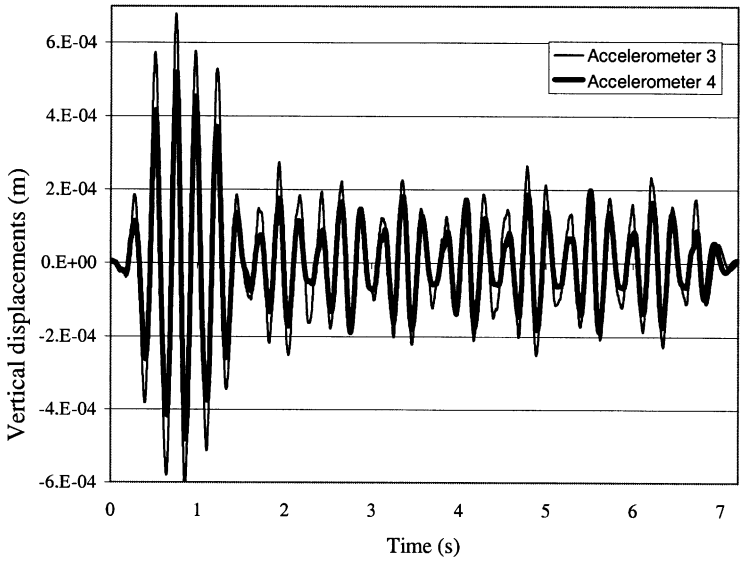

Fig. 12. Vertical displacements of ground surface in two perpendicular points near the track for a "Corail" train passage.

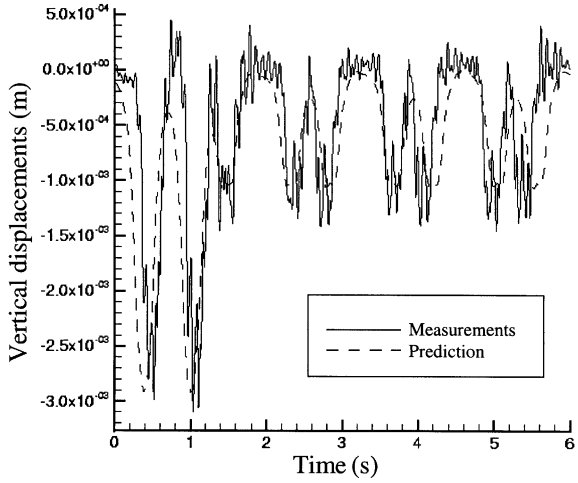

Fig. 13. Comparison of rail displacements between numerical model and VNR measurements.

According to the frequency of excitation different propagation modes appear in the layer for various types of wave.

The digital video analysis allows one to calculate absolute rail displacements against time at a chosen point between two sleepers during the passage of a train. The train is composed of an engine and six carriages and moves at 110 km/h. These results are compared to numerical results (2-D-model) in Fig. 13. For this qualitative study, the frequency of harmonic excitation is chosen to be equal to 15 Hz, corresponding to the maximum amplitude in the response spectra and close to the layer resonance.

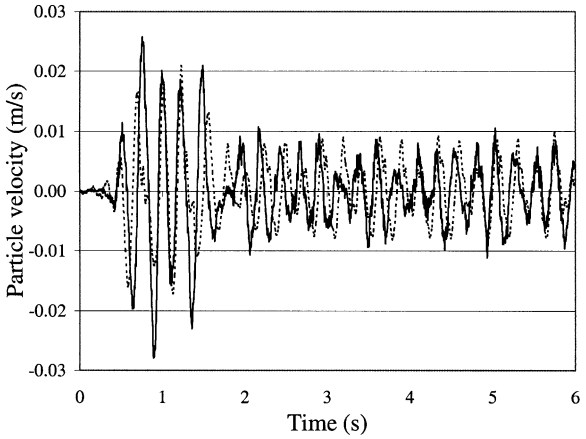

Fig. 14. Comparison of vertical particle velocities on soil at 2 m between (----) numerical model and (—) in situ measurements.

The acceleration of particles at the surface of the ground is measured along the track (at 2 m from the track) and particle velocities are calculated and plotted on Fig. 14. This signal can then be compared to the numerical result in the same figure. Maximum displacements can be found although the whole of the signal has not been taken into account. The passages of axles and bogies are correctly described by the numerical model. On the other hand, amplitudes are not exactly obtained. This difference comes from the several approximations in the numerical model, the difficulty to characterize track elements (especially the ballast) and the single frequency nature of each load in the model.

Other measurements at 2 or 5 m for different train configurations and for speeds of 70 or 110 km/ph were also compared. Except for a measuring error due to severe conditions during recording, results were able to validate the numerical model in the frequency range and for the mechanical parameters of soil described previously.

In fact, to deduce a complete response, contributions of the other frequencies of excitation are now missing. Therefore, in the framework of the linear model, it will be possible to include and superimpose responses due to the various excitations in order to obtain a better comparison.

7. Conclusions

A two-dimensional model of track–layered ground interaction has been developed for the study of low-frequency vibration in a railway system. This representation can easily be extended to a three-dimensional model allowing for validation between measurements and prediction at a distance from the track. The model takes into account the main linear parameters of the train, the track and the soil. In addition, in situ measurements have allowed an evaluation to be made of vertical and lateral displacements in the track and on the ground for different types of traffic and various speeds according to the speed range of the traffic on this railway line. The comparison can be done between numerical results and measurements despite some difficulties arising from in situ

measurements and from approximations in the two approaches. This agreement is good enough to conclude that the model allows credible information to be given on the track and soil behaviour.

Already these in situ measurements constitute a valuable database not only for this comparison but also to provide tools for estimations taking account of different traffic configurations and characteristics of the ground surrounding the railway track.

In the framework of this comparison, for the modified site where a control solution focused on a duplication of rails combined with a reduction of sleeper spacing, the measured attenuation of vibration (about 20%) has already been justified with the help of the numerical simulation.

In further work, some numerical implementations on the soil parameters will be carried out in order to reduce vibrations emitted from railway traffic. With this aim in view, a finite element model will be developed.

Acknowledgements

The authors wish to acknowledge the French Ministry of Environment for its financial support under research Grant No. DGAD/SRAE/99107 concerning the propagation of waves in ground due to a railway traffic moving at high speed.

References

[1] N. Chouw, G. Schmid (Eds.), *Proceedings of the International Workshop Wave* 2000, Bochum, Germany, A.A. Balkema, Rotterdam, 2000.

[2] G. Lefeuve-Mesgouez, Propagation d'Ondes dans un Massif Soumis à des Charges se Déplaçant à Vitesse Constante, Ph.D. Thesis, Ecole Centrale of Nantes, 1999 (in French).

[3] C. Madshus, A.M. Kaynia, High-speed railway lines on soft ground: dynamic behaviour at critical train speed, *Journal of Sound and Vibration* 231 (3) (2000) 689–701.

[4] G. Lefeuve-Mesgouez, A.T. Peplow, D. Le Houédec, Ground vibration in the vicinity of a high speed moving harmonic strip load, *Journal of Sound and Vibration* 231 (5) (2000) 1289–1309.

[5] G. Lefeuve-Mesgouez, D. Le Houédec, A.T. Peplow, Ground vibration due to high speed moving harmonical load, in: L. Fryba, J. Naprstek (Eds.), *Structural Dynamics—Eurodyn* 99, Vol. 2, A.A. Balkema, Rotterdam, 1999, pp. 963–968.

[6] H.A. Dieterman, A.V. Metrikine, The equivalent stiffness of a half space interacting with a beam. Critical velocities of a moving load along the beam, *European Journal of Mechanics* 15 (1) (1996) 67–90.

[7] X. Sheng, C.J.C. Jones, M. Petyt, Ground vibration generated by a load moving along a railway track, *Journal of Sound and Vibration* 228 (1) (1999) 129–156.